Definition of the near collapse in-plane drift capacity of rocking unreinforced masonry walls for the Dutch national guidelines

F. Messali, J.G. Rots
Delft University of Technology, the Netherlands

The in plane drift capacity of unreinforced masonry (URM) piers is an essential aspect in the seismic assessment of existing URM structures. Several empirical models are recommended in international codes, but none of them can accurately predict the drift at near collapse (NC) of URM piers that undergo rocking failure, also known as flexural failure. This work presents an update of an alternative empirical equation recently published by the authors. Starting from the original empirical equation, three correction factors are introduced (i) to account for the specific safety philosophy adopted by the Dutch guidelines NPR 9998, and also (ii) to consider the influence of alternative definitions of the NC drift capacity and (iii) of dynamic and short duration effects. The calibration process has been conducted by making use of a large dataset representative of Dutch clay and calcium silicate URM piers, and allowed for the identification of proper values of the correction factors. A final formulation of the empirical equation is presented. This formulation is currently recommended in NPR 9998.

Key words: Unreinforced masonry (URM), in-plane, drift capacity, calcium silicate masonry, clay brick masonry, empirical model

1 Introduction

Nonlinear analysis methods and displacement-based procedures have been used more and more in the assessment of existing unreinforced masonry (URM) buildings. It is often convenient to subdivide the structure into single components (piers, spandrels), and for each of these components define a proper behaviour under axial and shear loads. As regards URM piers, different failure mechanisms are traditionally distinguished: rocking, shear (sliding or diagonal cracking), and crushing. However, often a combination of these modes is observed (hybrid failure mode). Irrespective of the mechanism, the in plane drift capacity represents a crucial parameter for URM piers, since it is strongly related to the

performance of the building close to structural collapse, for both analytical methods and equivalent frame based models [e.g. Lagomarsino et al, 2013]. International standards often estimate the pier drift capacity via empirical equations and differentiate between the possible failure mechanisms (shear and rocking, alternatively denoted as flexure failure). Analytical mechanics-based formulations that relate the local deformation at material level to the global displacements of the structural element may represent an efficient alternative approach [e.g. Wilding and Beyer, 2017]. However, the analytical formulations in these models are very complex and still not validated for many specific masonry typologies. For this reason, simple empirical equations will be likely included in standards and guidelines also in the coming years. In case of rocking, standards often recommend the use of equations that include several physical parameters, the background of which is not always sufficiently transparent [Lu et al, 2016]. A summary of the empirical equations recommended in relevant international standards and guidelines is presented in Table 1, while the different parameters included in the models are listed in Table 2.

Table 1: Summary of the empirical equations recommended in international standards or guidelines to estimate the drift of masonry piers at near collapse

Standard/guideline	Recommended empirical equations	
EN 1998-3	$\delta_{u,EC8} = \frac{4}{3}\, 0.8\% \, \frac{H_0}{L}$	(1)
ASCE 41-13	$\delta_{u,ASCE} = \min\left(\frac{1}{2}\varepsilon_{cm}\left(\frac{\alpha\beta}{\sigma_o / f_c} - 1\right); 2.5\% \right)$	(2)
NZSEE 2017	$\delta_{u,NZSEE} = \frac{4}{3}\min\left(0.3\% \frac{H}{L}; 1.1\% \right)$	(3)
NTC 2018	$\delta_{u,NTC} = 1\%$	(4)
SIA D0237	$\delta_{u,SIA} = \begin{cases} \frac{4}{3}\, 0.8\% \, (1 - 2.4\frac{\sigma_o}{f_c}) & \text{for cantilever walls} \\ \frac{4}{3}\, 0.4\% \, (1 - 2.4\frac{\sigma_o}{f_c}) & \text{for double clamped walls} \end{cases}$	(5)

where: L, H, H_0 are the length, the height, and the effective height of the wall, respectively; σ_o the average overburden stress; f_c the mean compressive strength of masonry; ε_{cm} the ultimate compressive strain of masonry; a and β are parameters used to compute the neutral axis depth with the Whitney Stress Block for unconfined masonry (the value 0.85 is suggested [Priestley et al., 2007]).

In recent years few works proposed refined versions of the equations currently implemented in standards, specifically for hollow clay brick URM [Petry and Beyer, 2014a; Salmanpour et al, 2015], but there is still a lack of information for other masonry types. Recently, Messali and Rots [2018] presented an alternative empirical equation that applies for piers that undergo rocking or hybrid failure after the activation of a rocking mechanism. The equation was developed with specific attention to the characteristics of Dutch URM structural [Jafari et al, 2017] and material [Esposito et al, 2017] characteristics. The calibration was conducted by considering a dataset of tests performed on URM piers, including those part of a comprehensive testing program that aimed at the characterization of the structural behaviour of Dutch masonry carried out at the Macrolab/Stevinlaboratory of Delft University of Technology (TU Delft) [Messali et al. 2018] and at the European Centre for Training and Research in Earthquake (EUCentre) [Graziotti et al, 2018].

This paper presents an update of the empirical equation developed by Messali and Rots [2018]. First the characteristic of the experimental dataset used for the calibration work are described, and a comparison between the empirical equation presented by Messali and Rots [2018] and those recommended in international standards is provided. Then three correction factors are considered in addition to the original equation (i) to make it more suitable for the Dutch guidelines NPR 9998, (ii) to consider possible alternative definitions of the drift capacity at NC, and also (iii) to take into account the influence of dynamic effects and of short duration of the seismic inputs. Eventually, the amended formulation of the empirical equation is presented.

Table 2: Parameters evaluated in the models estimating the drift capacity of rocking URM piers in international standards

	EN 1998-3	ASCE 41-13	NZSEE 2017	NTC 2018	SIA D0237
Aspect ratio (H/L)	X		X		
Boundary conditions (H_0/H)	X			X	X
Axial load ratio (σ_0/f_c)		X			X

2 A dataset of quasi-static tests on rocking URM piers

The work of Messali and Rots [2018] considered a dataset of quasi-static tests performed on URM piers. The database consisted of 38 specimens, selected to be representative of the properties of Dutch masonry piers. The dataset included brick masonry walls (both clay and calcium silicate) characterised by low axial compressive loads (Figure 1a) and limited thickness. Different aspect ratios of the specimens were considered, being that related to the geometry of the piers in real buildings: calcium silicate masonry walls are used in terraced houses and have often large aspect ratios, while clay brick masonry walls can be used both in terraced and detached houses and therefore be both slender and squat (Fig. 1b). Only piers whose collapse is subsequent to the activation of a rocking mechanism were included in the list. In the original work of Messali and Rots [2018] the ultimate drift δ_u corresponding to the Near Collapse (NC) limit state was computed at the point of 20% strength degradation, as adopted previous works (e.g. by Petry and Beyer [2015], and by Salmanpour et al [2015]). However, there is no complete agreement among the scientific community and various approaches have been adopted by different researchers. In fact, the NC limit state as defined in EN 1998-3 [CEN 2005] should correspond to the condition of severe damage of the wall, that has low residual lateral strength and stiffness but it is able to withstand the vertical loads. In some of the considered tests, the specimens suffered progressive damage and they were able to sustain the vertical loads for imposed drifts much larger than those corresponding to 20% strength reduction. For this reason, in this paper two alternative definitions of the ultimate drift are presented: the first definition

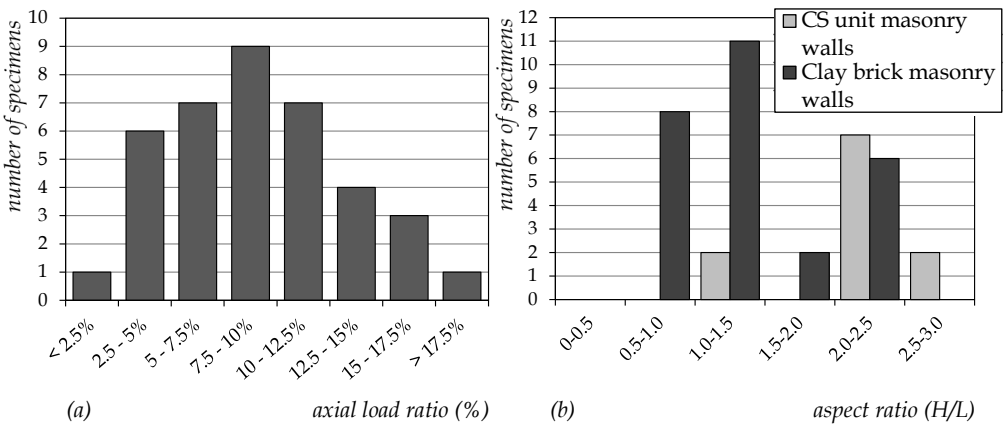

Figure 1. Distribution of specimens depending on their axial load ratio (a) or aspect ratio (b) [Messali and Rots 2018]

considers the drift at the point of 20% strength degradation ($\delta_{u,\text{at 20\% drop}}$), while the second definition assumes that the ultimate drift is equal to the largest imposed drift at which the pier was fully able to sustain the vertical loads ($\delta_{u,\text{ max drift}}$). In both cases, the average between the values obtained for positive and negative displacements is considered.

A summary of the main features of the tests grouped for different unit type is presented in Table 3, while Table 4 reports the main properties of the considered specimens: the employed masonry units, , the dimensions (length *L*, height *H*, thickness *t*), the ratio H_o/H H0/H, the applied confining vertical pressure σ_o , the mean masonry compressive strength f_c , the failure mode type, and the ultimate drift according to both the definitions discussed above ($\delta_{u,\text{at 20\% drop}}$ and $\delta_{u,\text{ max drift}}$).

3 Calibration of an empirical drift capacity equation

The empirical models recommended in international standards and guidelines identify the dependence of the ultimate drift on a number of parameters, such as the axial load ratio (σ_o/f_c), the aspect ratio (H/L), the boundary conditions (H_0/H). Additionally, the wall may depend also on a height factor (H_{ref}/H), while correction factors may be introduced in case of thin-layer mortar bed-joints or unfilled head-joints.

Of all the parameters introduced above, the calibration process carried out by Messali and Rots [2018] showed that only the axial load ratio, the aspect ratio and the height effect have

Table 3. Main features of the tests grouped for different unit types [Messali and Rots 2018]

	No. tests	H/L	σ_o/f_c	$\delta_{u,\text{at 20\% drop}}$
Clay bricks	27	1.33 ± 0.58	0.09 ± 0.05	1.72 ± 0.76 (CV = 44%)
Solid bricks	11	1.47 ± 0.65	0.05 ± 0.02	1.78 ± 0.82 (CV = 46%)
Perforated bricks	16	1.24 ± 0.53	0.12 ± 0.04	1.68 ± 0.75 (CV = 45%)
Calcium silicate units	11	2.19 ± 0.64	0.08 ± 0.02	1.72 ± 0.69 (CV = 40%)
Calcium silicate bricks	5	2.50 ± 0.00	0.09 ± 0.02	1.60 ± 0.57 (CV = 36%)
Calcium silicate blocks	4	1.50 ± 0.58	0.08 ± 0.00	1.35 ± 0.40 (CV = 30%)
Calcium silicate elements	2	2.81 ± 0.00	0.05 ± 0.00	2.77 ± 0.47 (CV = 17%)
Every specimen	38	1.58 ± 0.71	0.09 ± 0.04	1.72 ± 0.73 (CV = 43%)

Table 4. Database of quasi-static in-plane tests on rocking URM piers

name	ref	unit type	L	H	t	$\frac{H_0}{H}$	σ_o	f_c	fail mode	δ_u at 20% drop	δ_u max drift
			mm	mm	mm	-	MPa	MPa		%	%
W3	A	SC	1625	1625	198	1.12	0.31	6.2	R	0.78	0.78
18-1	B	PC	2500	1750	300	0.50	0.60	6.0	H	1.00	1.25
18-2	B	PC	2500	1750	300	0.50	0.60	6.0	H	1.00	1.50
18-3	B	PC	2500	1750	300	0.50	0.60	6.0	H	2.00	2.00
18-4	B	PC	2500	1750	300	0.50	0.60	6.0	H	1.22	1.50
15-1	B	PC	984	1250	300	1.18	1.18	7.0	H	1.64	1.80
15-5	B	PC	992	1170	300	1.18	0.94	5.5	R	2.04	2.04
15-8	B	PC	992	1170	300	1.18	0.89	5.2	H	3.32	4.27
10-1	B	PC	1028	1510	300	1.06	0.60	4.0	R	1.71	1.98
10-3	B	PC	1033	1510	300	1.06	0.60	4.0	H	1.31	1.66
10-6	B	PC	1026	1510	300	1.06	0.60	4.0	R	2.32	2.32
14-1	B	PC	2567	1750	297	1.10	0.56	4.0	H	1.37	1.71
CL01	C	PC	1500	2500	175	0.50	0.32	4.0	R	2.97	2.97
CL03	C	PC	1000	2500	365	0.50	0.15	3.9	R	1.48	1.48
CL06	C	PC	1250	2600	300	0.50	0.50	10.0	R	1.97	1.97
CS05	D	CS-BL	1250	2500	175	0.50	1.04	13.0	H	1.61	1.61
CS06	D	CS-BL	1250	2500	175	1.05	1.04	13.0	R	1.73	1.73
CS07	D	CS-BL	2500	2500	175	0.50	1.04	13.0	H	1.20	1.20
CS08	D	CS-BL	2500	2500	175	1.05	1.04	13.0	H	0.85	0.85
W-2.7-L1-a	E	SC	2700	2700	190	0.50	0.09	6.2	R	1.90	1.90
W-2.7-L2-a	E	SC	2700	2700	190	0.50	0.25	6.2	R	1.60	1.60
W-2.7-L2-b	E	SC	2700	2700	90	0.50	0.25	6.2	R	1.10	1.10
W-1.2-L2-a	E	SC	1200	2700	190	0.50	0.37	6.2	R	2.92	2.92
W-1.8-L2-a	E	SC	1800	2700	190	0.50	0.37	6.2	R	1.98	1.98
W-3.6-L2-a	E	SC	3600	2700	190	0.50	0.37	6.2	H	1.49	1.49
PUP3	F	PC	2010	2250	200	1.50	1.05	5.9	R	0.83	0.89
T7	G	PC	2700	2600	150	1.00	0.64	6.4	R	0.62	1.00
COMP-1	H	CS-BR	1100	2750	100	0.50	0.52	6.2	R	2.00	2.00
COMP2-1	H	SC	1200	2710	210	0.50	0.52	11.2	R	3.55	3.55
COMP2-2	I	SC	1200	2710	210	0.50	1.20	11.2	H	1.15	1.15

Table 4 continued

name	ref	unit type	L	H	t	$\frac{H_0}{H}$	σ_o	f_c	fail mode	δ_u at 20% drop	δ_u max drift
			mm	mm	mm	-	MPa	MPa		%	%
COMP2-3	I	SC	1200	2710	210	0.50	0.86	11.2	H	1.30	1.30
COMP-0a	J	CS-BR	1100	2750	100	0.50	0. 71	5.9	H	0.82	0.87
COMP-2	J	CS-BR	1100	2750	100	1.15	0.51	5.9	R	1.60	1.60
COMP-3	J	CS-BR	1100	2750	100	0.50	0.40	5.9	R	1.30	1.30
COMP-20	J	CS-BR	1110	2778	100	1.10	0.65	6.4	R	2.26	3.10
COMP-22	K	SC	2960	2710	210	1.10	0.36	9.24	H	1.81	1.81
COMP-24	K	CS-EL	977	2743	100	0.50	0.60	13.9	R	2.43	2.43
COMP-25	K	CS-EL	977	2743	100	1.10	0.60	13.9	R	3.10	3.10
Average			1683	2232	220	0.70	0.651	7.3	-	1.73	1.83

References: A = [Abrams et al, 1992], B = [Frumento et al, 2009], C = [Magenes et al, 2008a], D = [Magenes et al, 2008b], E = [Lee et al, 2008], F = [Petry et al, 2014], G = [Salmanpour et al, 2015], H = [Graziotti et al, 2016a], I = [Graziotti et al, 2016b], J = [Messali et al, 2019], K = [Esposito and Ravenshorst, 2017]

Materials: PC = Perforated clay bricks; SC = Solid clay bricks; CS-BR = Calcium silicate bricks; CS BL = Calcium silicate blocks; CS-EL = Calcium silicate elements.
Failure modes: R = Rocking failure; H = Hybrid failure.
δu, at 20% drop = drift at the point of 20% strength degradation.
δu ,max drift = maximum drift achieved by the specimen being able to withstand the vertical loads.

a statistical influence on the ultimate drift of the rocking walls, and the following empirical equation was proposed for the drift at 20% drop of the force with respect to the peak load:

$$\delta_{u,\text{ at 20\% drop}} = 1.6\% \left(1 - 2.6\frac{\sigma_o}{f_c}\right)\sqrt{\frac{H}{L}}\frac{H_{ref}}{H} \tag{1}$$

with H_{ref} assumed equal to 2.4 m, as suggested in [Petry and Beyer, 2015].

The accuracy of Equation 1 is compared to that of the empirical models recommended in international standards and guidelines and summarised in Table 1, by plotting the ratio between the predicted ($\delta_{u,p}$) and the experimental ($\delta_{u,e}$) ultimate drift at varying the axial load ratio. The results are plotted in Figure 2, along with the density curves of

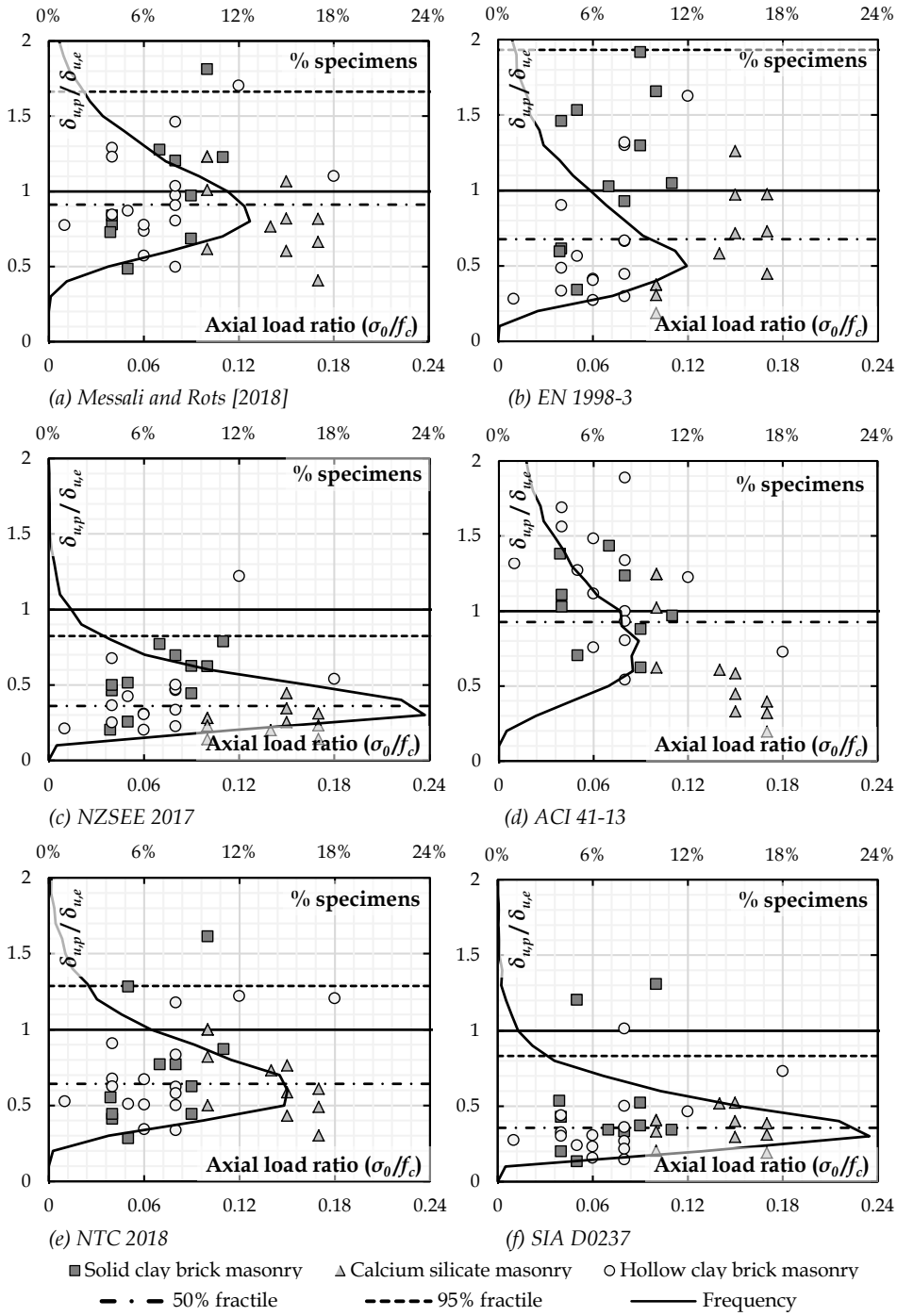

Figure 2. Predicted ($\delta_{u,p}$) over experimental ($\delta_{u,e}$) ultimate drifts at varying the axial load ratio for the empirical equation proposed in Messali and Rots [2018] and in international standards

equivalent distributions computed assuming a log-normal distribution of the sample (the equivalent distributions have a larger population to allow for a neater representation of the results). Optimal distributions should be lumped around the value one and show no trends. Besides, a limited dispersion of the results (i.e. a small coefficient of variation) is desirable. It should be noted that most of the considered standards, guidelines, and papers relate the displacement capacity to the pier failure mode.

It is important to stress that, since each empirical model targets different types of response, several specimens included in the considered dataset would not be recognised as rocking piers, and different equations would be used. Figure 3 plots the cumulative functions for both the original data and equivalent log normal distributions. Finally, Table 5 summarises the values of the mean average error (MAE), and the main statistics of the predicted over experimental ultimate drift ratios, being MAE defined according to Equation 2.

$$\mathrm{MAE} = \frac{1}{n}\sum_{i=1}^{n}\left|\delta_{u,p,i} - \delta_{u,e,i}\right| \tag{2}$$

Overall, the equation presented in Messali and Rots [2018] is the one with the best performance in terms of average results, dispersion and MAE. Among the other equations, a good performance is achieved by applying the moment-curvature based model suggested in [Priestley et al, 2007] in agreement with requirements of ASCE 41-13. The

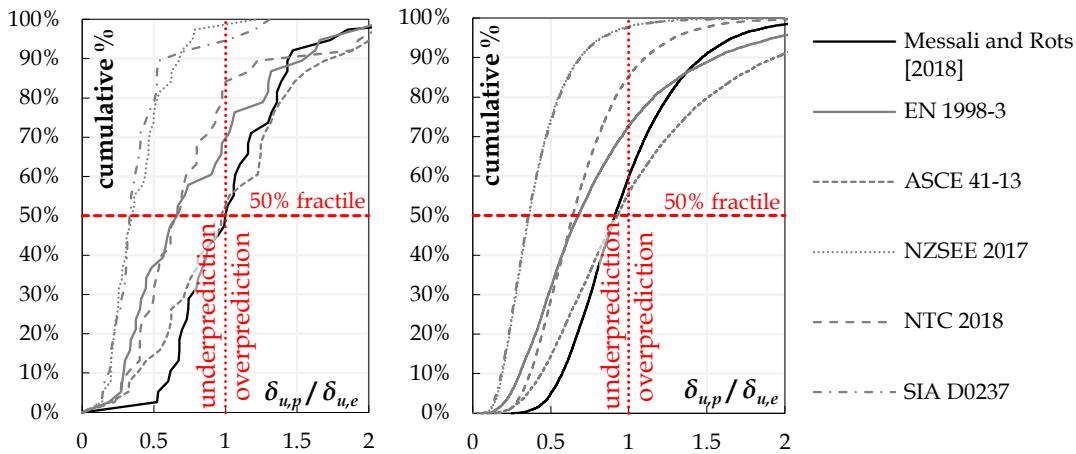

Figure 3. Cumulative functions of the predicted ($\delta_{u,p}$) over experimental ($\delta_{u,e}$) ultimate drift ratio for: (a) the original data and (b) an equivalent lognormal distributions of the considered dataset

average value is close to 1, and small values of MAE are obtained. However, a trend in the distribution of the predicted over experimental ultimate drift ratios seems to be identified (Fig. 2d), suggesting that the recommended hyperbolic dependence on the axial load ratio may lead to an underestimation of the displacement capacity of walls with large axial load ratio. It is interesting to note that the cumulative curves computed for NZSEE 2017 and SIA D0237 are extremely similar, even though one equation contains parameters that are neglected in the other one (as summarised in Table 2) and the individual estimates for each wall are often very different.

4 Correction factors to include the proposed formulation in NPR 9998

The calibration procedure used to define Equation 1 was performed considering a dataset of specimens selected to be representative of the properties of Dutch masonry piers, with the final goal of obtaining an empirical equation that may be included in the Dutch guidelines NPR 9998 for the assessment of existing buildings [NEN 2018]. However, the semi-probabilistic safety philosophy of NPR 9998 accepts an individual risk (i.e. the probability of death for a person as a consequence of an earthquake in the Groningen region) of 10^{-5} per year. A study of Martins et al. [2015] found probabilities of collapse of few percentage points for buildings designed to withstand low peak ground accelerations (PGA). For this reason, the capacity of a structure analysed assuming mean properties and loaded by design seismic loads is defined to have a 5% probability of global collapse [van Straalen et al, 2018]. The prediction of the pier drift capacity should be then calibrated so

Table 5. Main features of the tests grouped for different unit types

Standard/model	MAE	$\delta_{u,p}/\delta_{u,e}$			
	(%)	min	Max	μ	σ
Messali and Rots [2018]	0.50	0.41	2.17	0.97	0.39
EN 1998 3	0.79	0.19	2.16	0.83	0.51
ASCE 41-13	0.68	0.20	3.21	1.09	0.60
NZSEE 2017	1.07	0.14	1.22	0.41	0.22
NTC 2018	0.75	0.28	1.61	0.70	0.30
SIA D0237	1.13	0.13	1.31	0.41	0.26

MAE = mean absolute error; min = minimum value; Max = maximum value; μ = mean value; σ = standard deviation

that the fragility function of the global capacity of the building, to which the piers belong, has a conditional probability of collapse of 5% (in other words, the predicted capacity should overestimate the real capacity in no more than 5 out of 100 cases). Besides, the value of drift at NC is not uniquely defined in the literature, and the influence of available alternative definitions should also be assessed. Finally, the discussed dataset of experimental tests includes only quasi-static tests having a loading protocol (e.g. number and amplitude of the imposed horizontal cycles) that was developed to represent traditional tectonic earthquakes characterised by long shocks. On the opposite, the shallow earthquakes active in the Groningen province, which NPR 9998 relates to, are characterised by short duration and a reduced number of cycles compared to those of tectonic earthquakes. For this reason, a correction factor may be introduced to take into account the dynamic and short-duration effects.

Equation 1 can be then multiplied by a scalar coefficient A that is calibrated to account for the influence of the global 5% conditional probability of failure (A_0), the definition of the NC drift capacity (A_1), and the dynamic and short duration effects (A_2): $A = A_0 A_1 A_2$. The calibration of the coefficients A_0 , A_1 , and A_2 is discussed in the following sections.

*4.1 **Local and global safety (correction factor A_0)***

To be included in NPR 9998 the empirical equation must be calibrated so that the fragility function of the whole building has a conditional probability of failure equal to 5%. As first attempt, the same criterion defined at global (building) level has been applied directly at local (single pier) level, i.e. the equation is calculated so that only 5% of the predictions exceed the corresponding experimental value. In fact, this procedure associates the collapse of the building to that of the first pier, and it can be rather conservative. Depending on the geometry of the structure, a larger number of piers may collapse before the global failure of the building is achieved. It is difficult to estimate the corresponding probability of failure for the single pier, but it can be reasonably assumed to be smaller than 15%. For this reason, different values of the coefficient A_0 that lead to different cumulative curves and, as a consequence, different conditional probabilities of failure at local level have been considered (Fig. 4a). Figure 4b shows an almost linear dependency between the correction factor and the conditional probability of failure. For values of the latter between 5% and 15% A_0 varies between 0.60 and 0.75. An average value of 0.675 is then assumed.

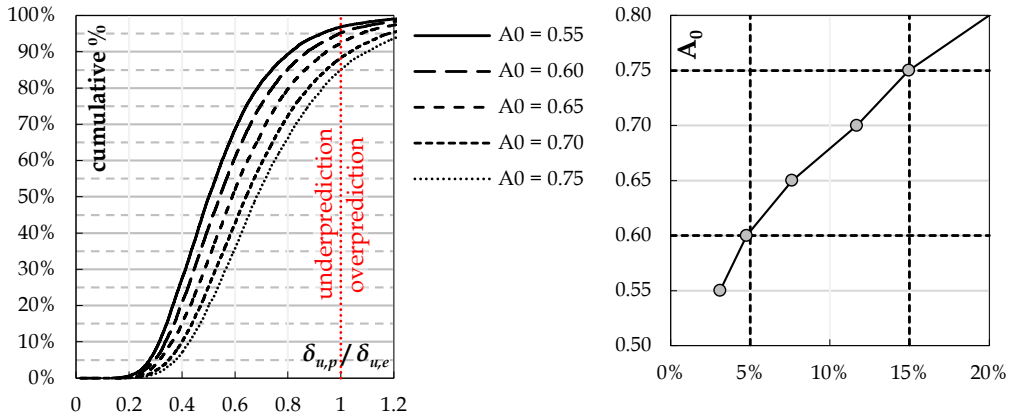

(a) ultimate drift ratio *(b) conditional probability of failure*

Figure 4. Cumulative functions of the predicted ($\delta_{u,p}$) over experimental ($\delta_{u,e}$) ultimate drift ratio (a) and conditional probability of failure (b) for different values of the scalar coefficient A_0

4.2 *Alternative definition of the NC drift (correction factor A1)*

Equation 1 was calibrated assuming that the NC drift corresponds to a post-peak drop of the shear force equal to 20% of the peak strength, in line with past literature [Petry and Beyer 2014, Salmanpour et al 2015]. However, no general consensus about the definition of NC drift is achieved amongst the scientific community. For this reason, two possible definitions of the NC drift capacity of the walls are considered: $\delta_{u,\text{at 20\% drop}}$ and $\delta_{u,\text{ max drift}}$, as defined in Section 2. While $\delta_{u,\text{at 20\% drop}}$ may be considered too conservative, on the other hand $\delta_{u,\text{ max drift}}$ exploits the maximum capacity of the specimen up to collapse. Both the values of $\delta_{u,\text{at 20\% drop}}$ and $\delta_{u,\text{ max drift}}$ for every specimen are reported in Table 4. In fact, two distinct groups of values are then obtained: the "$\delta_{u,\text{at 20\% drop}}$ values" and the "$\delta_{u,\text{ max drift}}$ values". On average the values in the two groups are close (the average NC capacity increases by 6%), and different NC drifts are found only for perforated clay brick masonry specimens and, to a lesser extent, for CS brick masonry piers. This observation is consistent with the experimental behaviour, since perforated clay and CS bricks usually undergo gradual compressive damage, eventually leading to the complete collapse of the walls. On the other hand, the compressive failure of large CS blocks or elements at the base of the pier usually occurs suddenly, and it determines a sudden loss of capacity of the pier and hence its complete collapse.

Figure 5 shows how the cumulative curves change when different correction factors A1 are considered. A smaller conditional probability of failure is computed for the $\delta_{u,\text{ max drift}}$

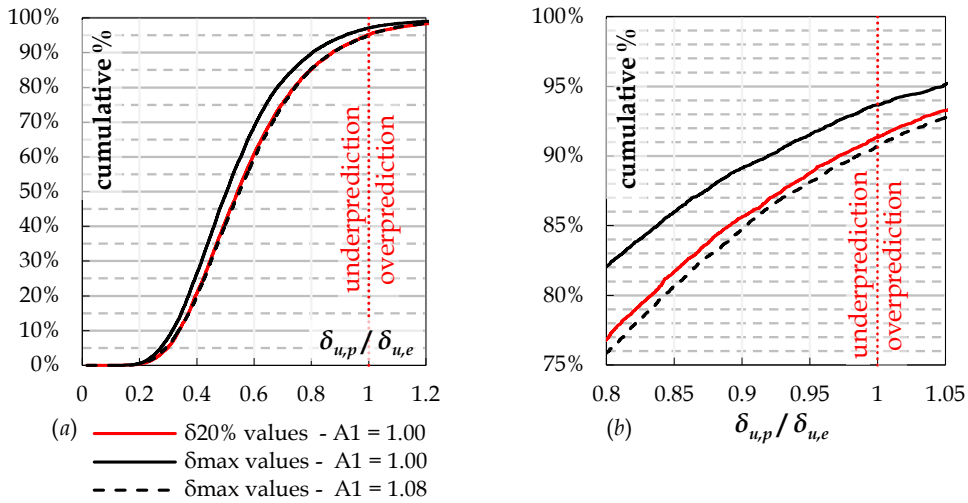

Figure 5. Cumulative functions of the predicted ($\delta_{u,p}$) over experimental ($\delta_{u,e}$) ultimate drift ratio for alternative definitions of the NC drift capacity and different values of coefficient A_1 (a). Detail of figure (a) for values of $\delta_{u,p}$ / $\delta_{u,e}$ around one (b).

values (6% vs 9%) if no correction factor is used. To obtain a similar probability of failure the correction factor A1 equal to 1.08 has to be applied.

4.3 *Dynamic and short-duration effects (correction factor A_2)*

Equation 1 has been derived considering quasi-static laboratory tests performed following loading protocols that are often not completely representative of real ground motions, since the number, amplitude and sequence of applied cycles follows standard schemes (e.g. Porter [1987], ATC-24 [1992]). Besides, the strain rates acting on walls during seismic events are much larger than those applied in quasi-static tests [Petry and Beyer, 2014]. The correction factor A_2 is then introduced to account for the influence on the displacement capacity of rocking URM walls of these two effects.

Regarding the influence of the loading protocol, specific comparisons at experimental level are presented by Petry and Beyer [2014a] and by Beyer et al. [2014]. During the experimental campaigns considered in these two papers, the ultimate drift achieved for monotonic tests is between two and three times the one obtained for cyclic tests. However, only specimens whose failure was mainly governed by shear were considered. More recent experimental and numerical works [Beyer and Mergos, 2015, Wilding et al., 2017] suggest

that, unlike walls governed by shear, the drift capacity of walls characterised by a rocking failure mode is not significantly affected by the applied loading protocol.

As regards the influence of the applied strain rate, few works [Williams and Scrivener, 1973, Tomazevic, 2000, Petry and Beyer, 2014b, Beyer et al., 2015] have analysed the difference in terms of outcomes between dynamic and quasi-static experimental tests. Overall, similar displacement capacity was obtained for walls tested in quasi-static or dynamic conditions. On the basis of the studies presented in this section, the value of a correction factor that accounts for dynamic and short-duration effects for rocking walls may be slightly larger than one, but not much larger. The value A_2 = 1.15 is assumed. This value falls within the range of values recommended for reinforced concrete by the US Department of Defense (2008) to account for the dynamic effects in elements subjected to an explosion. In any case, the data discussed above are not obtained by dedicated experimental campaigns, and future research on the influence of the loading history and of the strain rate on the NC drift capacity of URM piers is strongly advised.

4.4 Final formulation of the empirical equation

Based on the calibration analysis discussed in the previous sections, and assuming for sake of simplicity that the three correction factors are unrelated, a global factor $A \approx 0.85$ is suggested. When the correction factor A multiplies Equation 1, the following final formulation of the empirical equation is obtained:

$$\delta_u = 1.35\% \, (1 - 2.6\frac{\sigma_o}{f_c}) \sqrt{\frac{H}{L}} \frac{H_{ref}}{H} \tag{3}$$

The empirical equation has been included in NPR 9998:2018 (equation G.31) in the form presented in Equation 3.

5 Conclusions

This work presents an update of the empirical equation derived by Messali and Rots [2018] to estimate the NC drift capacity of rocking URM walls, so that the equation became ready to be included in the Dutch guidelines NPR 9998. In fact, the semi-probabilistic safety philosophy of these guidelines accepts an individual risk of 10^{-5} per year, that can be achieved when the fragility function of the capacity of the structure, to which the piers belong, has a 5% conditional probability of global collapse. Besides, the equation had to be

recalibrated to consider possible alternative definitions of the NC drift and the effect of the loading protocol (e.g. number of cycles and applied strain rate) on the displacement capacity of the piers.

The calibration process has been conducted by making use of the large dataset already analysed by Messali and Rots [2018], that was representative of Dutch clay and calcium silicate masonry URM piers. Starting from the original empirical equation, three correction factors are introduced to account for the influence of the global 5% conditional probability of failure (A_0), the definition of the NC drift capacity (A_1), and the dynamic and short duration effects (A_2). Assuming for sake of simplicity that these three correction factors are unrelated, a global factor $A = A_0 A_1 A_2 \approx 0.85$ is suggested. The empirical equation, including the correction factor A, is currently recommended in the Dutch guidelines NPR 9998 to estimate the drift capacity of URM piers that undergo rocking failure.

Acknowledgements

The research was supported by the Netherlands Standards Institute (NEN) and the Nederlandse Aardolie Maatschappij (NAM), which is gratefully acknowledged.

Literature

Abrams, D.P., Shah, N. (1992). Cyclic load testing of unreinforced masonry walls. Report #92-26-10. University of Illinois at Urbana-Champaign, USA.

ASCE, American Society of Civil Engineers (2014). Seismic Evaluation and Retrofit of Existing Buildings (ASCE/SEI 41 13). Reston, VA, United States.

ATC-24 (1992). Guidelines for cyclic seismic testing of components of steel structures for buildings. Applied Technology Council, California.

Beyer, K., and Mergos, P. (2015). Sensitivity of drift capacities of URM walls to cumulative damage demands and implications on loading protocols for quasi-static cyclic tests. In Proceedings of the 12th *North American Masonry Conference*.

Beyer, K., Petry, S., Tondelli, M., and Paparo, A. (2014). Towards displacement-based seismic design of modern unreinforced masonry structures. *Perspectives on European Earthquake Engineering and Seismology* (pp. 401-428), Springer.

CEN, European Committee for Standardisation (2005). Eurocode 8: Design of structures for earthquake resistance – Part 3: General rules, seismic actions and rules for buildings, Design Code EN 1998-3. Brussels, Belgium.

Esposito, R., Terwel, K.C., Ravenshorst, G.J.P., Schipper, H.R., Messali, F., Rots J.G. (2017). Cyclic pushover test on an unreinforced masonry structure resembling a typical Dutch terraced house. Proceedings of the 16th World Conference on Earthquake, 16WCEE.

Esposito, R., Ravenshorst, G. (2017). Quasi-static cyclic in-plane tests on masonry components 2016/2017. Delft University of Technology. Report number C31B67WP3-4, Final version, 10 August 2017.

Frumento, S., Magenes, G., Morandi, P., Calvi, G.M. (2009). Interpretation of experimental shear tests on clay brick masonry walls and evaluation of q-factors for seismic design. Technical report, IUSS PRESS, Pavia, Italy.

Graziotti, F., Rossi, A., Mandirola, M., Penna, A., Magenes, G. (2016a). Experimental characterization of calcium-silicate brick masonry for seismic assessment. Proceedings of the 16th *International Brick and Block Masonry Conference*, IBMAC.

Graziotti, F., Tomassetti, U., Rossi, A., Marchesi, B., Kallioras, S., Mandirola, M. et al. (2016b). Shaking table tests on a full-scale clay-brick masonry house representative of the Groningen building stock and related characterization tests. Report EUC128/2016U, EUCentre, Pavia, IT.

Graziotti, F., Penna, A., & Magenes, G. (2018). A comprehensive in situ and laboratory testing programme supporting seismic risk analysis of URM buildings subjected to induced earthquakes. *Bulletin of Earthquake Engineering*, 1-25.

Jafari, S., Rots, J.G., Esposito, R., Messali, F. (2017). Characterizing the material properties of Dutch unreinforced masonry. *Procedia Engineering*, 193: 250–7.

Lagomarsino, S., Penna, A., Galasco, A., Cattari, S. (2013). TREMURI program: an equivalent frame model for the nonlinear seismic analysis of masonry buildings. *Engineering Structures*; 56: 1787-1799.

Lee, J.H., Li, C., Oh, S.H., Yang, W.J., Yi, W.H. (2008). Evaluation of rocking and toe crushing failure of unreinforced masonry walls. *Advances in Structural Engineering*, 11(5): 475–89.

Lu, S., Beyer, K., Bosiljkov, V., Butenweg, C., D'Ayala, D., Degee, H., et al. (2016). Next generation of Eurocode 8. Proceedings of the 16th *International Brick and Block Masonry Conference*, IBMAC.

Magenes, G., Morandi, P., Penna, A. (2008a). Experimental In-plane cyclic response of masonry walls with clay units. Proceedings of the 14th *World Conference on Earthquake Engineering*, 14WCEE.

Magenes, G., Morandi, P., Penna, A. (2008b). D7.1c Test results on the behaviour of masonry under static cyclic in-plane lateral loads. Pavia, Italy: ESECMaSE.

Martins, L., Silva, V., Crowley, H., Bazzurro, P., Marques, M. (2015). Investigation of Structural Fragility for Risk-targeted Hazard Assessment, 12th International *Conference on Applications of Statistics and Probability in Civil Engineering*, ICASP12, Vancouver, Canada.

Messali, F., Rots, J.G. (2018). In-plane drift capacity at near collapse of rocking unreinforced calcium silicate and clay masonry piers. *Engineering Structures*; 164: 183-194.

Messali F., Esposito R., Jafari, S., Ravenshorst, G.J.P, Korswagen, P. and Rots J.G. (2018). A multiscale experimental characterisation of Dutch unreinforced masonry buildings. Proceeding of 16th *European Conference on Earthquake Engineering* (ECEE), Thessaloniki, Greece.

Messali, F., Esposito, R., Ravenshorst, G., Rots, J.G. (2019). Experimental investigation of the in-plane cyclic behaviour of calcium silicate brick masonry walls. *Bulleting of building engineering* (submitted)

MIT, Ministry of Infrastructures and Transportations (2018). NTC 2018. Aggiornamento delle Norme Tecniche per le Costruzioni. Supplemento ordinario alla "*Gazzetta Ufficiale*, (42) (in Italian).

NEN, Nederlands Normalisatie Instituut (2018). NPR 9998:2018 nl. Beoordeling van de constructieve veiligheid van een gebouw bij nieuwbouw, verbouw en afkeuren - Geïnduceerde aardbevingen - Grondslagen, belastingen en weerstanden. Delft, the Netherlands (in Dutch).

NZSEE, New Zealand Society for Earthquake Engineering (2017). The seismic assessment of existing buildings, Part C8: Seismic assessment of unreinforced masonry buildings. Wellington, New Zealand: MBIE, EQC, SESOC, NZSEE and NZGS.

Petry, S. and Beyer, K. (2014a). Influence of boundary conditions and size effect on the drift capacity of URM walls. *Engineering Structures*, 65, pp. 76-88.

Petry, S., and Beyer, K. (2014b). Review and improvement of simple mechanical models for predicting the force-displacement response of URM walls subjected to in-plane loading. 2nd *European Conference on Earthquake Engineering and Seismology*.

Petry, S., Beyer, K. (2015). Influence of boundary conditions and size effect on the drift capacity of URM walls. *Engineering Structures*; 65: 76-88.

Porter, M.L. (1987). Sequential phased displacement (SPD) procedure for TCCMAR testing. 3rd meeting of the joint technical coordinating committee on masonry research, US-Japan coordinated program.

Priestley, M.J.N., Calvi, G.M., Kowalski, M.J. (2007). *Displacement-Based Seismic Design of Structures*, Pavia: IUSS Press.

Salmanpour, A.H., Mojsilović, N., Schwartz, J. (2015). Displacement capacity of contemporary unreinforced masonry walls: an experimental study. *Engineering Structures*; 89: 1-16.

Swiss Society of Engineers and Architects SIA (2011). SIA D0237: Evaluation de la sécurité parasismique des bâtiments en maçonnerie. Zürich, Switzerland (in French)

Tomazevic, M. (2000). Some aspects of experimental testing of seismic behavior of masonry walls and models of masonry buildings. *ISET Journal of earthquake Technology*, 37(4): 101-117.

US Department of Defense (2008). UFC 3-340-02. Unified Facilities Criteria (UFC): Structures to Resist the Effects of Accidental Explosions. Washington D.C., USA.

van Straalen, J., Steenbergen, R.D.J.M., Vrouwenvelder A.C.W.M. (2018). Background Report NPR 9998:2018 - Part A: Terminology and Safety Philosophy. TNO Report: TNO 2018 R10254. 9 October 2018.

Wilding, B., Beyer, K. (2017). Force–displacement response of in-plane loaded unreinforced brick masonry walls: the Critical Diagonal Crack model. *Bulletin of Earthquake Engineering*; 15(5): 2201-2244.

Wilding, B.V., Dolatshahi, K.M., and Beyer, K. (2017). Influence of load history on the force-displacement response of in-plane loaded unreinforced masonry walls. *Engineering Structures*, 152: 671-682.

Williams, D., and Scrivener, J.C. (1973). Response of reinforced masonry shear walls to static and dynamic cyclic loading. Proceedings of the 5th *World conference on earthquake engineering*, Rome, Italy.